Effect of densification rate on consolidation and properties of Al7075–B_4C composite powder

G. H. Majzoobi[1], A. Atrian[2] and M. K. Pipelzadeh*[3]

Hot quasi-static pressing and dynamic compaction of Al7075–B_4C composite powder are studied in this work. Micron sized Al7075 and B_4C particles were milled to obtain uniform dispersion of B_4C reinforcing phase. Samples with relative densities up to 97.5, 99 and 100% were fabricated using gas gun, drop hammer and hot quasi-statically compactions respectively. The results showed that the increase of B_4C content improved the hardness of the compacts but did not improve the compressive strength in the samples compacted by the gas gun. However, the ductility of the samples was reduced significantly. The samples compacted using the drop hammer and under hot quasi-static loading experienced ~25 and 11% enhancement in the compressive strength respectively. The investigation indicated that the dynamic compaction using the gas gun was more successful if it is performed after quasi-static pre-compaction and under warm compaction process. It was concluded that the quasi-static pressing is the best fabrication technique to achieve the highest density, microhardness and strength.

Keywords: Boron carbide (B_4C), Al7075 powder, Quasi-static compaction, Dynamic compaction, Gas gun

Introduction

Aluminium matrix composites are widely used in industries such as aerospace, automotive, microelectronics and military applications due to their excellent properties and their high strength/weight ratio.[1] Among the aluminium matrix composites, aluminium-7075 with excellent mechanical properties has received more attention especially in the aerospace industry. The properties of this alloy can be improved by reinforcing it with hard ceramic particles such as SiC, Al_2O_3, B_4C and TiB_2 using different powder metallurgy (PM) processes. The reinforced aluminium alloy enjoys the properties of a metal such as strength and high toughness and the properties of a ceramic such as high temperature and wear resistance.[2] Various PM techniques such as hot pressing and hot extrusion, which employ quasi-static loading and different dynamic compaction processes, can be used for the fabrication of the composites. Dynamic or shock wave consolidation is one of the techniques that use the energy of an impact for powder densification. The main advantage of the dynamic compaction techniques is that hot sintering is usually eliminated from the production cycle and it is replaced by the cold sintering. The dynamic compaction techniques usually use the gases due to the explosion or compressed gases as propellant to accelerate a projectile for the compaction of the powder or the use of the impact of a dropping hammer for this purpose.[3] Unlike the conventional powder densification techniques, the dynamic processes offer the possibility of producing the high temperatures necessary for particle metallurgical bonding, precisely where it is required, while the powder remains relatively cool elsewhere. Therefore, in the dynamic compactions techniques, the microstructural changes such as particle agglomeration and grain growth, which may happen due to the high temperature rise, can be minimised.[4]

In some investigations, the consolidation of various powders has been accomplished using the shock wave induced in the compact by a gas gun[5–7] or explosive[8] facilities. Dai and Thadhani[7] studied the shock compression response of the magnetic nano-Fe_3O_4 powder. They compacted the powder using a three-capsule, plate impact, gas gun set-up at the impact velocities up to 1100 m s^{-1}. Fredenburg *et al.*[6] consolidated 6061-T6 aluminium powder using a single stage light gas gun at a velocity of ~730 m s^{-1}. Hernández *et al.*[5] also used shock compaction technique for the fabrication of Al–Ni_3Al composite. Gu and Ravichandran[9] obtained Hugoniot data for some ceramic powders such as Al_2O_3 using plate impact experiments by a single stage powder gun.

In the presented work, Al7075–B_4C composite is produced by the warm dynamic compaction using a single stage gas gun and mechanical drop hammer, and

[1]Mechanical Engineering Department, Bu-Ali Sina University, Hamedan, Iran
[2]Department of Mechanical Engineering, Najafabad Branch, Islamic Azad University, Isfahan, Iran
[3]College of Engineering, Swansea University, Singleton Park, Swansea SA2 8PP, UK

*Corresponding author, email kazimp@student.icws-uk.co.uk

Published by Maney on behalf of the Institute
Received 01 February 2015; accepted 10 April 2015
DOI 10.1179/1743290115Y.0000000008

also by quasi-static hot pressing using an Instron universal testing machine. The compaction tests using gas gun are conducted with and without pre-compaction. Moreover, the effects of the volume fraction of reinforcing phase on the density, compressive behaviour, microhardness and microstructural behaviour of the specimens are investigated.

Experimental

Materials

Al7075 powder as the matrix (gas atomised, -100 μm, irregular morphology, Khorasan Powder Metallurgy Co., Iran) and B_4C as the reinforcing particles (average 10–100 μm, nearly spherical morphology) were milled in a planetary ball mill at room temperature and in the inert argon atmosphere. The milling media consisted of 22 hardened chromium steel balls with a diameter of 10 mm confined in a 125 mL steel vial. The milling process was performed at a rotation speed of 300 rev min^{-1} and took $\sim$2 h. About 30 g of the powder mixture along with 0.5 mass-% of stearic acid as process control agent, to decrease the unwanted adhesion, were subjected to the milling.[10] The number and total weight of the steel balls were also chosen in a way to attain more collisions between the balls and the powders and to achieve a ball/powder mass ratio of 3:1 respectively. Phase identification of the samples during milling was performed by X-ray diffraction (XRD) using a Philips X'PERT PW3040 diffractometer (40 kV/30 mA) with Cu K_α radiation ($\lambda = 0.154059$ nm). The scanning angles were also between 10 and 90°.

Fabrication of composite samples

In order to study the effects of the rate of compaction loading, the composite samples were fabricated under quasi-static and dynamic loadings. Five grams of different powders Al7075, Al7075–5 vol.-% B_4C, and Al7075–10 vol.-% B_4C with initial density of $\sim$55% of the theoretical density were selected for these processing techniques. MoS_2 high temperature die wall lubricant was also used to minimise the frictional force of the die and to improve the surface quality of the samples. The samples were then ground and polished for examination by optical microscopy and scanning electron microscopy (SEM). TESCAN field emission SEM (FESEM) was used to observe microstructure and compaction quality of the samples. Energy dispersive spectroscopy (EDS) analysis (1.2 nA beam current, 10 000 × magnification) prepared by SEM-TESCAN could also detect different elements inside the samples. Density measurement was made using the Archimedes principle.

In order to remove any remaining defects such as microcrack, a post-compaction sintering was also performed on the specimens. This treatment was performed at 873 K for 105 min in air, and the samples were wrapped by an aluminium foil (to prevent oxidation). To evaluate the compressive behaviour of the compacted samples, a number of compressive tests were conducted at a strain rate of $\sim 0.008\ s^{-1}$ using a 60 tons Instron testing machine. The Vickers microhardness of samples was also measured by applying a 100 gf to the specimen for 15 s using a tetragonal indenter. The samples were produced under three different loading conditions: (i) quasi-static pressing, (ii) dynamic compaction using drop hammer and (iii) dynamic compaction using gas gun.

Quasi-static hot pressing

Before starting the quasi-static tests, it was necessary to obtain the optimised conditions of hot pressing process to reach the highest density.[11] Parameters such as the magnitude and duration of pressure application on density were examined. In this regard, four Al7075 specimens without nano-reinforcement were hot pressed at 698 K and in a uniaxial die under the conditions given in Table 1. It must be mentioned that this examination was carried out only to find the best conditions for the hot pressing. The results of this examination are not among the main results of the work.

As the table suggests, a compaction pressure of 500 MPa applied for 30 min can lead to the highest density. Therefore, this pressure and its time duration were designated to fabricate the main samples with 0–10 vol.-% B_4C reinforcement. The rate of loading was selected to be 5 mm min^{-1}, which created strain rates $\sim 8.0 \times 10^{-3}\ s^{-1}$ in the samples. In order to avoid pore formation, the pressure on the specimen was removed when the compaction temperature fell below 573 K.[11,12] It should be mentioned that we may get higher densities at higher pressures, but the problem is that the stresses induced in the die and the punch due to very high pressure may significantly exceed the stress levels that can be tolerated by the materials of the punch and the die and lead to their severe damage. This remark has also been observed by most researchers in their investigations. In fact, they ignored 1–2% increases in the density to protect their die against damages due to the high pressures. The quasi-static hot pressing was conducted on a 60 tons Instron testing machine.

Dynamic compaction using drop hammer

A mechanical drop hammer was used for the compaction process of the composite powder. The drop hammer utilises a 60 kg falling weight to reach the impact velocity of 8 m s^{-1} ($v = \sqrt{2gh}$) for a free falling height of 3.5 m. It can be worked out that this impact velocity produces a strain rate of $1.0 \times 10^3\ s^{-1}$ and 2 kJ energy ($E = mv^2/2$), which is delivered to the powder for compaction. The weight is selected to produce the highest density for the samples. A schematic view of the drop hammer is illustrated in Fig. 1. Here, the compaction was performed at 698 K and without quasi-static pre-compaction. More details about this process also can be found in previous studies.[2,13] For this type of tests, it was necessary to examine the stress induced in the die components and the pressure of the compaction. This is explained in the section 'Finite element analysis of the impact'.

Table 1 Different processing conditions in hot quasi-static pressing

Relative density/%	Time/min	Pressure/MPa	Test no.
96.60	15	250	1
96.72	30	250	2
97.50	15	500	3
97.84	30	500	4

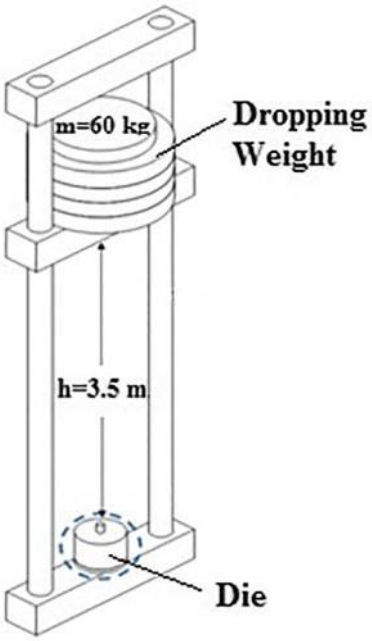

1 Schematic view of mechanical drop hammer

Dynamic compaction using gas gun

A single stage gas gun with compressed air as propellant, 100 mm bore diameter and 3 m long barrel supplied the required impact loading for the compaction. About 180 bar pressure, which is released by means of a pneumatic actuated valve and tearing of a PTFE diaphragm, could accelerate a 1.05 kg projectile up to 160 m s^{-1} velocity. This impact velocity corresponds to a strain rate of $\sim 1.6 \times 10^4$ s^{-1} and produced $\sim$12 kJ energy, which was delivered to the powder for the compaction. For this type of tests, it was necessary to examine the stress induced in the die components and the pressure of the compaction. This is explained in the next section.

In dynamic test using gas gun, the powder is compacted by impacting a projectile shot by the gas gun on the die, which is mounted on a rigid anvil. The disc shape projectile is made from St37 steel and has a diameter of 80 mm and a length of 20 mm. The projectile is mounted in a 100 mm diameter and $\sim$300 g PTFE sabot (*see* Fig. 2). The sabot keeps the projectile horizontal during the firing inside the launch tube and enables the operators to adjust the required tolerance between the projectile and the launch tube. The dynamic compaction using the gas gun can be accomplished in two ways depending on the impact velocity. At low impact velocities, say of the order of few hundred meters per second, which is the case in this investigation ($\sim$150 m s^{-1}), the energy of the projectile is delivered to the compact, and this energy is responsible for the compaction of the powder. However, at high impact velocities of the order of typically $>$500 m s^{-1}, the stress waves induced by the impact of the projectile are responsible for the compaction of the powder.[6,7] In this work, a punch die assembly was designed for the compaction of the powder. The components of the assembly are depicted in Fig. 2. The die was made of 1.2344 heat treated hot work tool steel. A shock resisting steel punch made of the steel 1.2542 with a diameter of 15 mm was also used to transfer the impact energy from the projectile to the powder. Two 5 mm thick disc shape tablets made of the punch material and with the same diameter were placed beneath and on the top of the powder to reduce the spring back effect of the specimen and to improve the compaction procedure.[14]

In order to avoid the movement of the die by the impact of the projectile, the die was supported by a 50 mm thick plate, which can be regarded as a rigid wall against the impact of the projectile. The die support and the details of the die are shown in Fig. 3.

The flyer plate (the projectile) impact on the punch induces a stress waves that travel down the punch towards the powder. A perpendicular impact between the flyer plate and the punch gives rise to a one-dimensional propagation of shock wave through the powder without being attenuated.[7] Therefore, the test equipments such as the gas gun launch tube, the projectile sabot assembly, the die and its supporting plate, and the die components should be aligned and be set up in a way to guarantee a perpendicular impact between the punch and the flyer plate. The tolerance between the two 5 mm thick tablets (*see* Fig. 3*b*) and the internal diameter of the die cavity is of great importance and the effect of bulging that may occur in the tablets due to the impact must be taken into account. If the tolerance is overdesigned, the powder would escape from the gap between the die and the tablets during the impact, leading to less densification of the compact. For underestimated tolerances, the tablets would stick to the die's wall (because of bulging) and the upper tablet is prevented from free movement and consequently the powder would not be compacted properly. By trial and error, the best tolerance for the fabrication of samples with highest relative density was determined as 0.2–0.3 mm. Similar comments can be made for the tolerance between the punch and the die cavity.

Moreover, when a powder is heated up to a certain temperature, its yield stress and strain hardening reduces

2 Projectile and compaction set-up used in gas gun assisted compacted samples

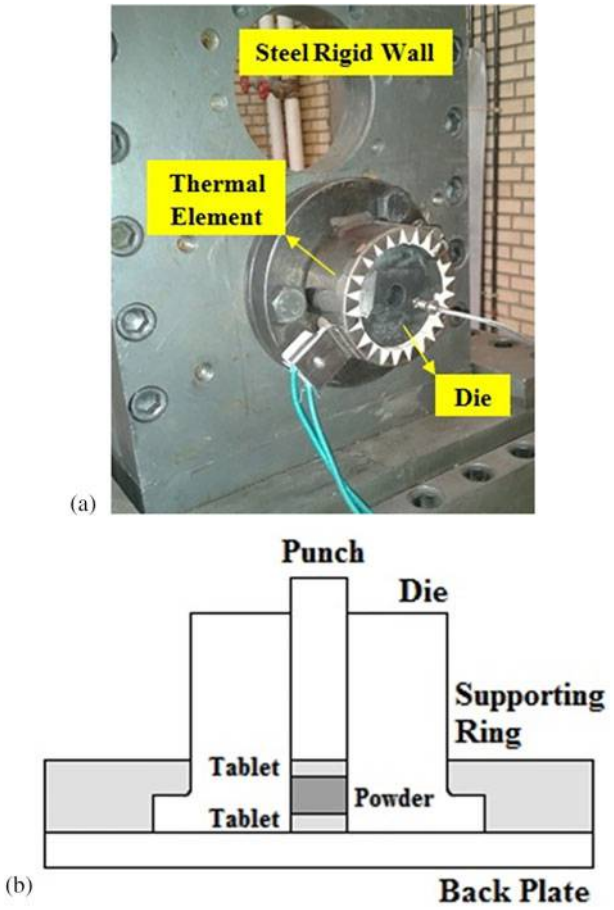

3 ***a*** **die support assembly;** ***b*** **schematic view of die set-up**

and the material becomes more ductile. Therefore, higher values of relative density can be reached compared with the compaction at room temperature. The experimental results also indicated that compaction at room temperature did not yield desirable results. Under this compaction conditions, the compacted samples were cracked, leading to fragmentation and highly porous compact with the maximum density of ~90% without enough particle bonding. Therefore, all compaction tests were carried out at 573 K using a 1000 W ceramic heating element (*see* Fig. 3*a*). In order to examine the effect of pre-compaction on the final compact quality, some of the samples were pre-compacted up to 77% of relative density. This initial compaction of powder was carried out quasi-statically using a hydraulic press machine.

Finite element analysis of impact

Before starting the dynamic tests using the gas gun, we had to obtain some information about the maximum stress level to which the die components are subjected on one hand and the pressure required for densification of the powder to reach the maximum compaction on the other. The maximum stress and pressure are consequences of the impact velocity. It was important to obtain the range of the impact velocity without damaging the die on one hand and obtaining the maximum allowable pressure for compaction on the other. High pressure gives high density but induces high stress levels, which may damage the die components. Therefore, a compromise should have been made between the compaction pressure and the stress levels in the die components. We made some numerical simulations using a commercial finite element code and pretests to examine the relation between the impact velocity, densification pressure and the stress levels induced in the die components. These pretests were necessary to be done before starting the main experiments and designing the die and the test set-up. Two-dimensional finite element (FE) simulation using AUTODYN software was employed to predict the stress histories at different locations in the sample and the die set. The non-linear dynamic analysis was performed for a 2D axisymmetric model and was solved explicitly. A powder compaction model known as equation of state is an essential requirement for the simulation of powder compaction. All equations of the state define the relation between volume and pressure. There is variety of models available in the softwares for this purpose. In this work, the p–α equation of the state[15] was employed for the numerical simulations. The basic form of this equation is a polynomial in P, given as follows[16]:

$$\alpha = \alpha_0 + \alpha_1 P + \alpha_2 P^2 + \alpha_3 P^3 \quad (1)$$

In this equation, P is the compaction pressure, α_0 to α_3 are the calibrated coefficients, and α is the porosity that is related to the compaction density and is defined as follows[15]:

$$\alpha = \frac{V}{V_S} = \frac{\rho_S}{\rho} \quad (2)$$

where V and ρ are the specific volume and density of the porous material respectively. V_s and ρ_s are the specific volume and density of its corresponding solid material. The P–α model was obtained from the load–displacement curve of the powder compaction under quasi-static loading and is shown in Fig. 4.

The FE analysis showed that the peak pressure of incident stress in the punch loaded by the gas gun and drop hammer compaction are ~2.2 and 1 GPa respectively. This stress varies within the compact and causes powder particles to be bonded. Figure 5 depicts the contours of the induced axial stress along the impact direction in the model.

Results and discussion

In this section, the characteristics of the composite powder before compaction are studied using XRD, SEM and EDS. The microstructure of the compacted composite powder is also investigated using SEM and the hardness measurement and by performing compression test on the specimens. These results are provided in the next sections.

Composite powder characteristics

Figure 6 shows the Al7075–B_4C composite powder after 2 h of mechanical milling. The grey regions seen on the Al particles are B_4C particles settled over the Al particles. This is indicated by EDS point analysis depicted in Fig. 6*c*. As the figure indicates, the B_4C particles are larger than other nano-reinforcements, and as a result, they are not distributed homogeneously between the Al particles, which are considerably larger than the B_4C particles. Generally, the nano-sized particles are preferred in the case of obtaining more uniform distribution

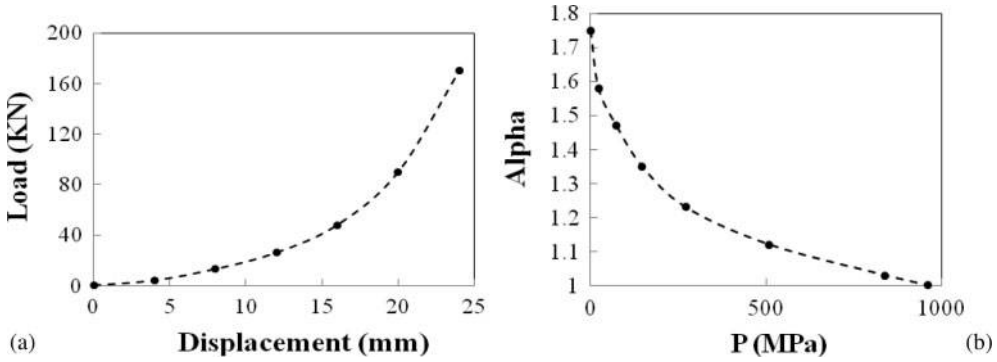

4 Compaction behaviour of Al7075 powder (*a*) used to define *p*–α model for numerical simulations (*b*)

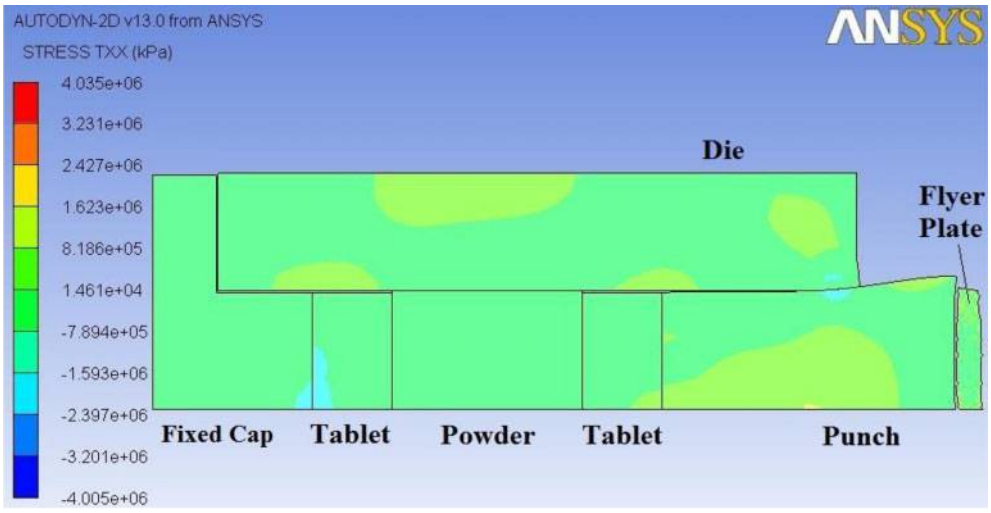

5 Contours of axial stress induced by impact using gas gun

between the matrix particles.[13] The XRD analysis of the composite powder indicated that the milled powder includes only Al and B_4C and no new phase were produced as a result of milling. These may be attributed to the short duration of the milling.

Bulk composite characteristics

The XRD analysis for the compacted samples also shows no new phases created through the consolidation process. Of course, XRD can just reveal phases that take a certain volume fraction. Therefore, thin interaction layers between Al and B_4C may need to be identified by techniques such as TEM. However, since TEM needs specimens with thickness <100 μm, because of porous nature and the lack of full sintering of the specimens, it was not possible to prepare such thin specimens.

In the dynamic compaction process and according to the energy equation $E=mv^2/2$, the kinetic energy delivered to the specimen increases as the impact velocity increases. Therefore, the fine particles are easily pushed into pores between the coarse particles, leading to the reduction of the porosity and the increase in the green density.[3] Density is one of the measures to qualify the consolidation of powder materials. The properties of a composite depend not only on the properties of the matrix itself but also on the reinforcement material and its interaction with the matrix. Volume fraction of hard phase particles in a multiphase microstructure is the most important factor affecting the density and mechanical properties such as the strength and fracture toughness.[17] Variation of relative density of compacted samples versus volume fraction of B_4C is presented in Fig. 7. The maximum compaction densities achieved for each of compaction using the gas gun, drop hammer and quasi-static pressing is 97.5, 99 and 100% respectively. As the figure indicates, the variation exhibits a reducing trend for the gas gun assisted compacted samples when B_4C content increases from 0 to 10 vol.-%, while, for the hot quasi-static pressing, this trend is increasing and, for the drop hammer compacted samples, a uniform variation cannot be observed. In general, quasi-static hot pressed samples show higher relative density than dynamically compacted ones. This is obviously due to the longer time duration of exposing pressure and temperature in the hot pressing, while in the dynamic compaction, the compaction is performed in a very short period of time. Generally, compaction and sintering of composite materials are different from those of the monophase materials. The presence of hard and non-deformable particles in a ductile matrix reduces the press-ability of the material.[17] Porosities in the compacted sample in Fig. 8*a* demonstrate this behaviour.

Figure 8 shows SEM image of Al7075–10 vol.% B_4C composite compacted using a single stage gas gun (relative density $\sim$96%) and at an impact velocity of 140 m s^{-1}. This figure shows Al grains in the microstructure of the sample. As it is known, the relative density is the ratio of compact density to theoretical

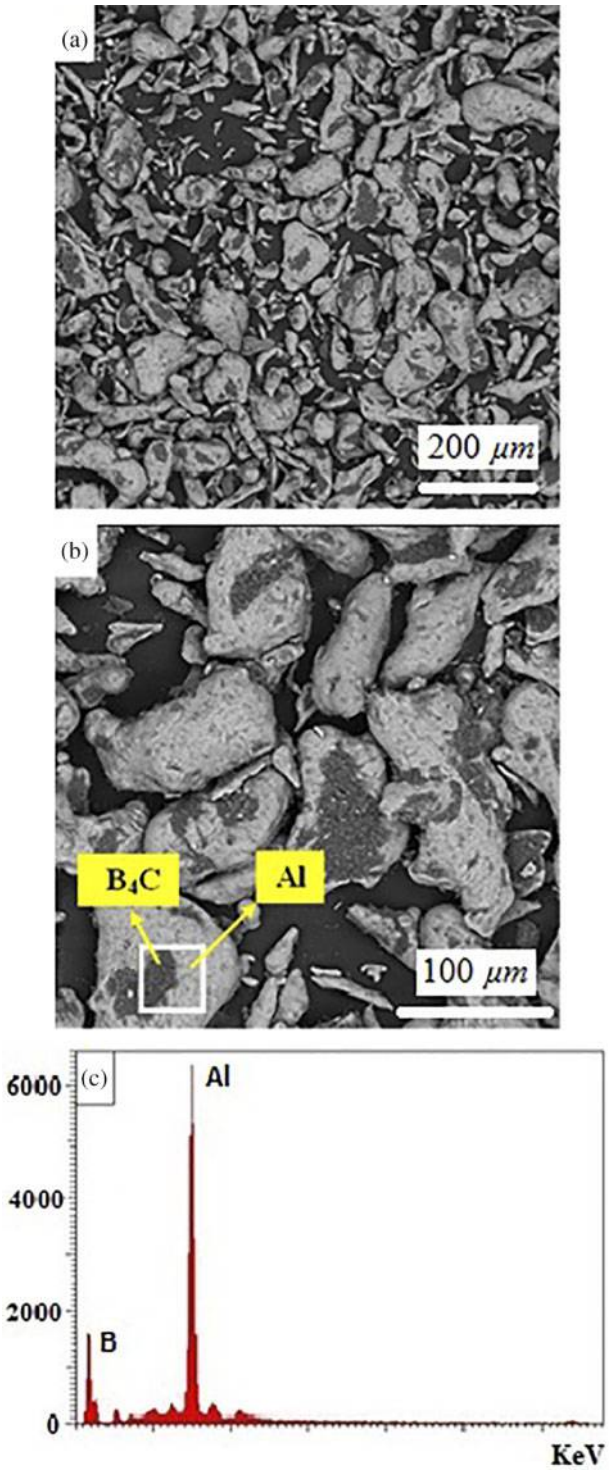

6 *a*, *b* FESEM backscattered micrograph of 2 h milled Al7075–5 vol.-% B_4C composite powder in two magnifications; *c* EDS point analysis of pointed dark region in (*b*)

density of the material. Reinforcing Al7075 with a density of 2812 kg m^{-3} by different volume fractions of B_4C with a density of 2520 kg m^{-3} reduces the final composite theoretical density based on the rule of mixture (theoretical density of Al7075–5 vol.-% B_4C and Al7075–10 vol.-% B_4C is calculated as 2797 and 2782 kg m^{-3} respectively). As demonstrated by equation (3), for Al7075–B_4C composite samples, the numerator and the denominator reduce and so the ratio does not have a definite trend. Therefore, as observed for the drop

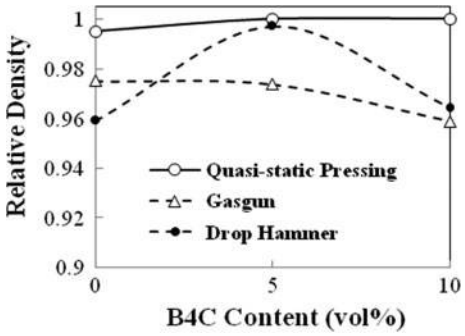

7 Variations of relative density versus B_4C volume fraction for three processing techniques

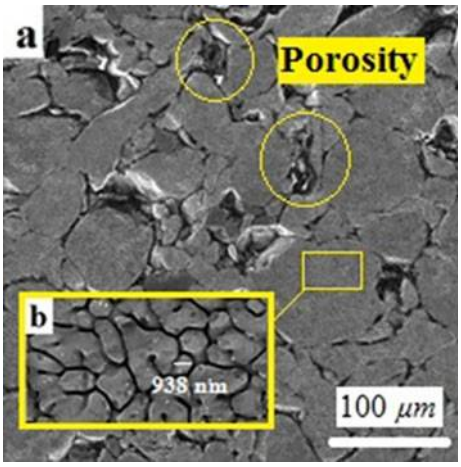

8 *a* SEM image of compacted Al7075–10 vol.-% B_4C composite by single stage gas gun (relative density ~96%) and impact velocity of 140 m s^{-1}; *b* microstructure of sample showing Al grains

hammer compacted samples, this ratio can be either increasing or decreasing and is dependent on the rate of the variation of the compact and theoretical density.

$$\rho_{Relative} \updownarrow = \frac{\rho_{Compact} \downarrow}{\rho_{Theory} \downarrow} \tag{3}$$

The variations of Vickers microhardness versus B_4C volume fraction are illustrated in Fig. 9. The figure clearly indicates that the hardness slightly increases with the increase of B_4C content for all of the compaction techniques. The results also reveal that the hardness of

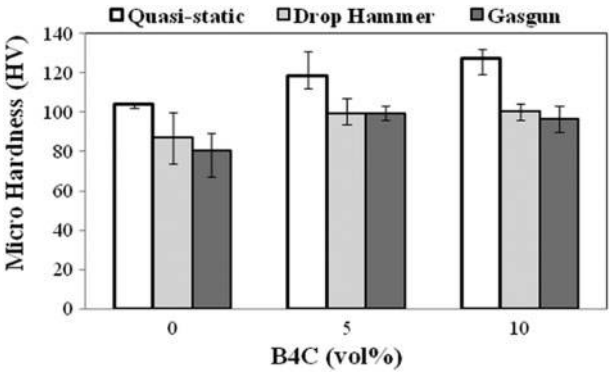

9 Variations of Vickers microhardness versus B_4C volume fraction for three processing techniques

quasi-statically pressed samples is typically 20% higher than that of the dynamically compacted specimens. This is obviously due to the stronger particle bonding in the quasi-static hot pressing. The hardness improvement is another indication of the material strength improvement too. This improvement is due to the second phase hardening effects of added phase and its intrinsic hardness.[18] Similar observations have already been reported by Alizadeh and Taheri-Nassaj[18] and Dong *et al.*[19]

The compressive true stress–strain curves of the Al7075–B_4C composites for different B_4C contents were obtained from a number of compression tests. The results are depicted in Fig. 10. As it is observed, a maximum increase of ~11% in the strength of the compaction is obtained for the specimen with 10% B_4C and compacted under hot quasi-static pressing (*see* Fig. 10*a*). The strength improvement for the drop hammer compacted samples can be seen in Fig. 10*b*, is ~25% and is generally lower than the corresponding curves in Fig. 10*a*. For the gas gun assisted compacted samples (Fig. 10*c*), however, the addition of B_4C to the aluminium not only does not make any improvement in the composite strengths but gives rise to ~10% reduction (for 10% B_4C) in the strength too. Figure 10*d* compares the compressive strength obtained in the considered methods.

For all of the compaction techniques, the addition of B_4C reduces the ductility of the samples. The reason for ineffectiveness of the reinforcing phase on the compressive behaviour of the dynamically compacted composites may be due to the non-uniform dispersion of B_4C and the weak bonding of the particles, which may occur during the short duration of an impact with a low energy. This is why, in hot pressed samples, both of the elastic modulus and the strength improve with the increases in B_4C content. A few investigations[19,20] have also reported undesired effects of the second phase reinforcement. Ahmed *et al.*[20] used cold and hot isostatic pressing and hot extrusion to fabricate the Al7075–SiC nanocomposite. They observed a significant drop in the hardness and tensile properties of the samples and attributed this behaviour to Mg segregation at the oxidised Al–SiC_{np} interfaces and grain boundaries.

The effect of quasi-static pre-compaction in dynamic consolidation using the gas gun was also investigated in this work. Figure 11 depicts the effect of pre-compaction on the dynamic compaction process and final sample quality. As this figure suggests, the perfect sample with the length and diameter of 8–9 mm and 15 mm respectively has been produced using a pre-compaction process. A compacted sample without pre-compaction is also presented in the figure. The imperfect sample suffers from delaminating and fragmentation and is generally not fully compacted such that most of it remains in powdery status after the impact. Basically, in the dynamic compaction process, due to the very high velocity of compaction, the air trapped between the particles has not enough time to escape. This gives rise to the formation of voids inside the powder. The voids in turn become the barrier against the full densification of the powder. Therefore, with one-stage compaction, high density will not be obtained. In order to eliminate this deficiency, at the beginning and before conducting the dynamic compaction, the powder is usually pre-compacted by quasi-static pressing to compress out the trapped air slowly. Then, the pre-compacted specimen is subjected to the dynamic compaction process.[21]

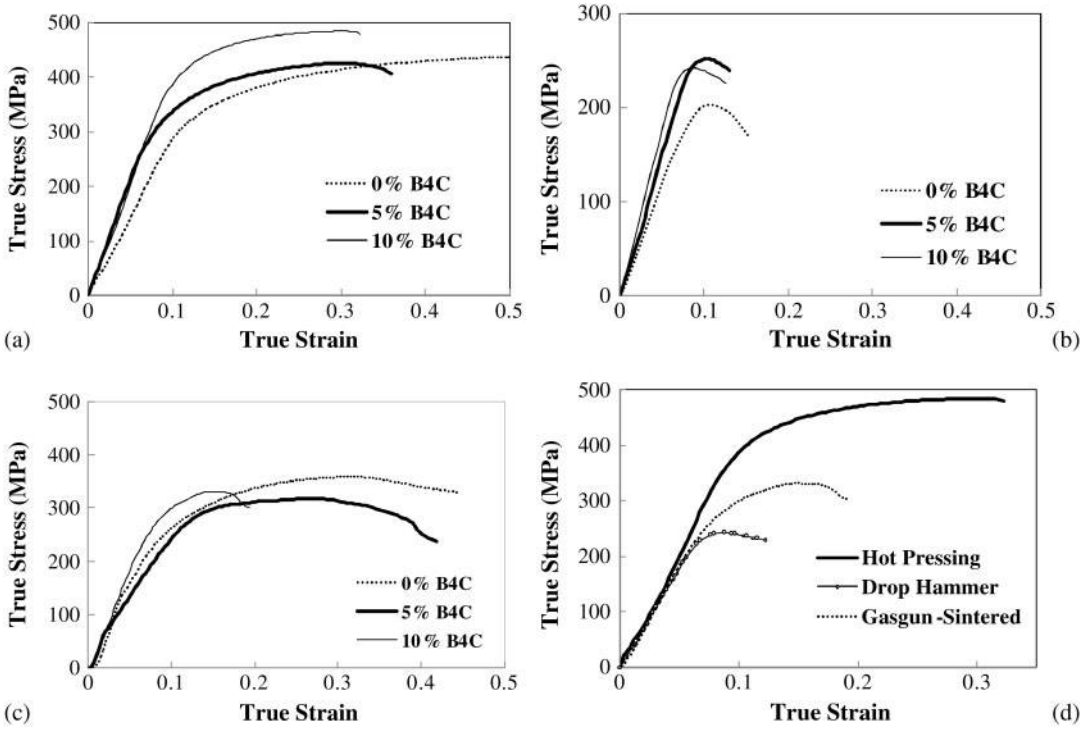

10 Compressive behaviour of Al7075–B_4C composite samples fabricated by *a* quasi-static hot pressing, *b* dynamic compaction using drop hammer, *c* dynamic compaction using gas gun, and *d* comparison between different processing methods for Al7075–10 vol.-% B_4C samples

11 Pre-compaction effect on quality of compacted samples using gas gun

Conclusions

From the results of this investigation, the following conclusions may be drawn:

1. Reinforcing Al7075 with B_4C using gas gun compaction method reduces the relative density by ~1.5%. This parameter, for the quasi-static pressing, has increasing trend, and for the drop hammer compaction, a consistent behaviour cannot be observed.

2. The relative density of quasi-static pressed compacts is higher than the dynamic ones due to the longer time duration of being exposed to pressure and temperature.

3. The microhardness of Al7075–B_4C composites increases by ~15–22% with respect to the monolithic material for the employed processing techniques. The microhardness of the compacted specimens was higher for the quasi-static pressing than those obtained from the gas gun and drop hammer assisted techniques.

4. Incorporating B_4C particles in Al7075 matrix enhances the compressive strength ~11 and 25% for the quasi-static hot pressed and drop hammer assisted compacted samples respectively. For the dynamic compaction using the gas gun, the strength reduces by ~9%.

5. The highest compressive strength was obtained for the quasi-static pressing.

6. In order to produce perfect samples in the dynamic compaction process, the powder must be pre-compacted by quasi-static compaction.

References

1. S. A. Khadem, S. Nategh and H. Yoozbashizadeh: *J. Alloys Compd*, 2011, **509**, 2221.
2. A. Atrian, G. H. Majzoobi, M. H. Enayati and H. Bakhtiari: *Int. J. Miner. Metall. Mater.*, 2014, **21**, 295.
3. J. Z. Wang, X. H. Qu, H. Q. Yin, M. J. Yi and X. J. Yuan: *Powder Technol.*, 2009, **192**, 131.
4. W. H. Gourdin: *Prog. Mater. Sci.*, 1986, **30**, 39.
5. P. Hernández, H. Dorantes, F. Hernández, R. Esquivel, D. Rivas and V. López: *Adv. Powder Technol.*, 2014, **25**, 255.
6. D. A. Fredenburg, N. N. Thadhani and T. J. Vogler: *Mater. Sci. Eng. A*, 2010, **A527**, 3349.
7. C. Dai and N. N. Thadhani: *Acta Mater.*, 2011, **59**, 785.
8. C. T. Wei, E. Vitali, F. Jiang, S. W. Du, D. J. Benson, K. S. Vecchio, N. N. Thadhani and M. A. Meyers: *Acta Mater.*, 2012, **60**, 1418.
9. Y. B. Gu and G. Ravichandran: *J. Impact Eng.*, 2006, **32**, 1768.
10. C. R. B. L. Kollo, R. Veinthal, C. Jäggi, E. Carreno-Morelli and M. Leparoux: *Mater. Sci. Eng. A*, 2011, **A528**, 6606.
11. M. Jafari, M. H. Abbasi, M. H. Enayati and F. Karimzadeh: *Adv. Powder Technol.*, 2012, **23**, 205.
12. M. Tavoosi, F. Karimzadeh, M. H. Enayati and A. Heidarpour: *J. Alloys Compd*, 2009, **475**, 198.
13. A. Atrian, G. H. Majzoobi, M. H. Enayati and H. Bakhtiari: *Adv. Powder Technol.*, 2015, **26**, 73.
14. B. Azhdar, B. Stenberg and L. Kari: *Polym. Test.*, 2005, **24**, 909.
15. W. Herrmann: *J. Appl. Phys.*, 1969, **40**, 2490.
16. J. P. Borg, D. J. Chapman, K. Tsembelis, W. G. Proud and J. R. Cogar: *J. Appl. Phys.*, 2005, **98**, 073509.
17. S. S. Razavi-Tousi, R. Yazdani-Rad and S. A. Manafi: *Mater. Sci. Eng. A*, 2011, **A528**, 1105.
18. A. Alizadeh and E. Taheri-Nassaj: *Tribol. Lett.*, 2011, **44**, 59.
19. Y. L. Dong, F. M. Xu, X. L. Shi, C. Zhang, Z. J. Zhang, J. M. Yng and Y. Tan: *Mater. Sci. Eng. A*, 2009, **A504**, 49.
20. A. Ahmed, A. J. Neely, K. Shankar, P. Nolan, S. Moricca and T. Eddowes: *Metall. Mater. Trans. A*, 2010, **41A**, 1582.
21. M.-J. Yi, H.-Q. Yin, J.-Z. Wang, X.-J. Yuan and X.-H. Qu: *Front. Mater. Sci. China*, 2009, **3**, 447.